Journal of Computer-Aided Molecular Design, **15:** 235–245, 2001.
KLUWER/ESCOM

Force-field parametrization and molecular dynamics simulations of *p*-menthan-3,9-diols: a family of amphiphilic compounds derived from terpenoids

Adriana M. Namba[a,†], Salvador León[b], Gil Valdo José da Silva[a] & Carlos Alemán[b,*]
[a]*Departamento de Quimica da Faculdade de Filosofia Ciência e Letras de Ribeirão Preto, Universidade de São Paulo, Av. Bandeirantes No. 3900, 14040-901, Ribeirão Preto, SP, Brazil;* [b]*Departament d'Enginyeria Química, E.T.S. d'Enginyers Industrials de Barcelona, Universitat Politècnica de Catalunya, Diagonal 647, Barcelona E-08028, Spain*

Received 23 December 1999; accepted 17 October 2000

Key words: cyclohexyl derivatives, force-field parametrization, molecular dynamics, p-menthan-3,9-diols, terpenoids

Summary

A set of amphiphilic *p*-menthan-3,9-diols have been investigated by molecular dynamics simulations. These are four stereoisomers than can be specifically obtained from two terpenoids widely used in biorganic chemistry. For this purpose, the *p*-menthan-3,9-diols have been explicitly parametrized using both semiempirical and ab initio quantum mechanical calculations. The reliability of these parameters has been validated by predicting different molecular and thermodynamic properties. Molecular dynamics simulations in aqueous solution have been performed with the new parameters. The results provide useful insights about the conformational properties of this family of compounds and the formation of intra- and intermolecular hydrogen bonds.

Introduction

When a bulky substituent on a cyclohexane ring is in axial position, it suffers repulsive interactions with the axial hydrogens. The free energy difference between equatorial and axial conformers provides a quantitative measure of such interactions that is related with the size of the substituent. Thus, the conformational analysis of substituted cyclohexane rings has been a subject of intensive research for many years [1, 2]. More recently, polar groups have instigated a particular interest as versatile substituents of adjustable bulk and potential hydrogen bonding capability. Thus, the conformational properties of cyclohexane rings bearing polar substituents like for example amino [3, 4], amide [5] and hydroxyl [6–8] groups have recently been elucidated.

On the other hand, the study of amphiphilic alkanediols is becoming an interesting topic of research due to their tendency to aggregate to supramolecular systems. Thus, recent studies have revealed that linear *n*-alkane-1,2-diols with a chain length $n > 5$ show monotropic mesophases which can be stabilized by the addition of water [9]. Moreover, molecular mechanics (MM) and molecular dynamics (MD) simulations on cyclohexyl substituted 1,2-ethanediols clusters in aqueous solution supports the formation of bilayer-like structures [10]. However, the effect of the close hydroxyl groups on the conformational properties of cyclohexyl ring were not examined.

We are interested in the conformational properties of *p*-menthan-3,9-diols, which consist of a cyclohexane ring bearing methyl, hydroxyl and 1-methyl-2-hydroxyethyl substituents at C1, C3 and C4, respectively (Scheme 1).

This family of compounds can be obtained from two terpenoids usually used in the synthesis of natural

*To whom correspondence should be addressed.
E-mail: aleman@eq.upc.es
†On leave to the Universitat Politécnica de Catalunya.

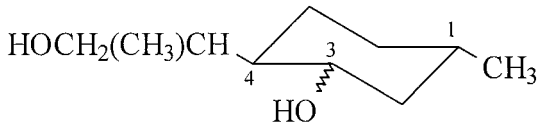

Scheme 1.

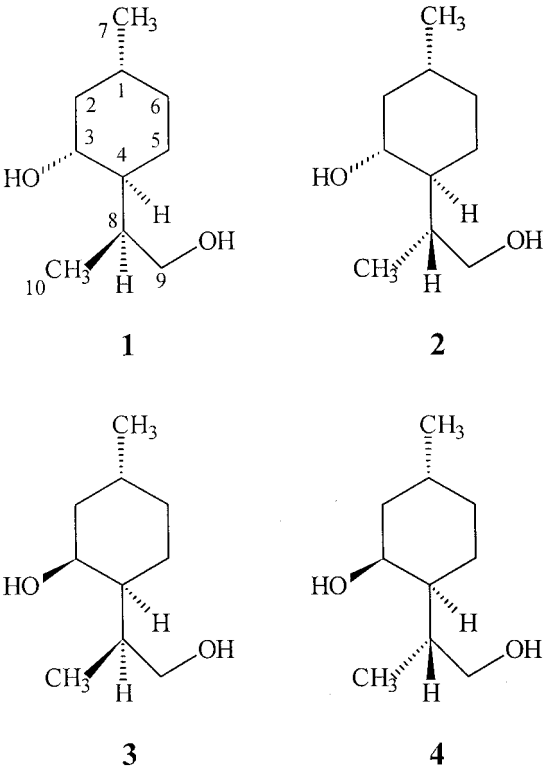

Scheme 2.

products, called isopulegol and *neo*-isopulegol [11]. The two hydroxyl groups contained in *p*-menthan-3,9-diols are close in the space conferring them an amphiphilic character and allowing the formation of intramolecular hydrogen bonds. Furthermore, these molecules present four asymmetric centers, three of them in the cyclohexane ring, which spreads their interest from a structural point of view.

In this article we present both an explicit force-field parametrization and the MD simulation results in aqueous solution of the four stereoisomers that can be specifically obtained from (−)-isopulegol and (+)-*neo*-isopulegol. These are the (1R:3R:4S:8S)-*p*-menthan-3,9-diol (**1**), (1R:3R:4S:8R)-*p*-menthan-3,9-diol (**2**), (1R:3S:4S:8S)-*p*-menthan-3,9-diol (**3**) and (1R:3S:4S:8R)-*p*-menthan-3,9-diol (**4**) (Scheme 2).

The paper is organized as follows. In the next section we present the force-field parameters explicitly developed for this study. Such parameters were validated by comparing the molecular geometries and thermodynamic data obtained from MM with those provided by ab initio quantum mechanical calculations. This comparison is displayed in the same section. After this, the computational procedure used in MD simulations is explained. Then, the MD results obtained in aqueous solution for the four stereoisomers are presented. Finally, in the last section summarizes our findings.

Force-field parametrization

In recent MM and MD studies of cyclic molecules [12–14] we found that excellent results can be achieved using simple harmonic force-fields, even for highly strained rings [14], if a suitable explicit parametrization of the system under study is performed. For this study we have developed an explicit parametrization for *p*-menthan-3,9-diols using quantum mechanical calculations. Classical energies have been computed using the analytical potential function of the Amber force-field [15]. In detail it presents the following functional form:

$$\begin{aligned} E_{ff} = {} & \Sigma_{bonds}\, K_r(r_{ij} - r_{ij}^{eq})^2 + \Sigma_{angles} K_b(\theta_{ij} - \theta_{ij}^{eq})^2 \\ & + \Sigma_{dihedrals}\, V_n/2[1 + \cos(n\varphi - \gamma)] \\ & + \Sigma_{nonbonded}\, q_i q_j/\varepsilon r_{ij} + \Sigma_{nonbonded}[A_{ij}/r_{ij}^{12} \\ & - B_{ij}/r_{ij}^{6}] + \Sigma_{H-bonds}[C_{ij}/r_{ij}^{1}2 - D_{ij}/r_{ij}^{1}0] \quad (1) \end{aligned}$$

In the above equation, the first term represents covalent bond stretching, the second describes bond angle bending, while the third are the dihedral interactions. The last three terms of the force-field energy describe the non-bonded interactions: electrostatic, van der Waals and 12–10 H-bond [15]. A complete set of stretching (K_r and r_{ij}^{eq}), bending (K_b and θ_{ij}^{eq}), torsional (V_n and γ) and nonbonding (q_i, q_j, A_{ij}, B_{ij}, C_{ij} and D_{ij}) parameters has been determined for *p*-menthan-3,9-diols. The atom types needed to develop the force-field are displayed in Figure 1.

Stretching, bending and torsional terms

The four *p*-menthan-3,9-diols investigated were fully optimized at the ab initio HF/6-31G(d) level [16]. The optimized geometries were used to determine the equilibrium bond distances (r_{ij}^{eq}) and angles (θ_{ij}^{eq}), which are displayed in Table 1. The stretching (K_r) and

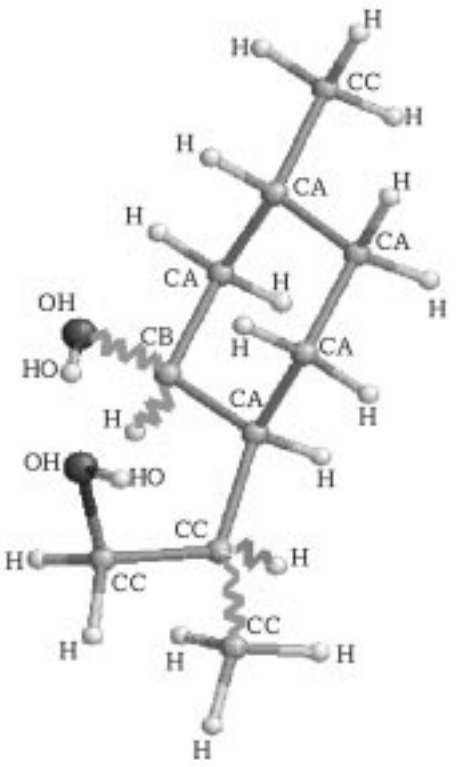

Figure 1. Atom types assigned to the *p*-menthan-3,9-diols.

Table 1. Equilibrium bond distances (r_{ij}^{eq}, in Å) and angles (θ_{ij}^{eq}, in degrees), and stretching (K_r, in kcal mol Å^2) and bending (K_b, in kcal/mol rad^2) force parameters for *p*-menthan-3,9-diols (atom types are indicated in Figure 1).

Stretching	r_{ij}^{eq}	K_r	Bending	θ_{ij}^{eq}	K_b
CA-CA	1.531	432	CA-CA-CA	111.8	85
CA-CB	1.540	370	CA-CA-CB	113.0	85
CA-CC	1.549	387	CA-CA-CC	114.8	82
CA-H	1.081	364	CA-CA-H	110.2	50
CB-H	1.089	364	CA-CB-CA	111.2	78
CB-OH	1.414	434	CA-CB-H	108.4	45
CC-CC	1.534	354	CA-CB-OH	106.2	84
CC-H	1.086	364	CA-CC-CC	114.8	75
CC-OH	1.406	434	CA-CC-H	106.1	65
OH-HO	0.945	458	CB-CA-CC	112.7	85
			CB-CA-H	109.2	45
			CB-OH-HO	110.1	67
			CC-CA-H	106.3	51
			CC-CC-CC	110.6	70
			CC-CC-H	110.2	53
			CC-CC-OH	111.1	84
			CC-OH-HO	109.4	67
			H-CA-H	106.5	46
			H-CB-OH	107.3	59
			H-CC-H	107.3	39
			H-CC-OH	109.8	49

bending (K_b) force constants were derived from semi-empirical AM1 calculations [17]. Thus, a systematic work comparing stretching and bending force parameters derived from HF/6-31G(d,p), MP2/6-31G(d,p), MP4/6-31G(d,p) and AM1 calculations with the experimental ones revealed that the latter method provides results of similar quality to the MP4/6-31G(d,p) ones [14]. The computed stretching and bending force constants, which are also reported in Table 1, were obtained using the standard PAPQMD strategy [18, 19]. According to this method, each bond and angle type was perturbed from its equilibrium geometry. The quantum mechanical energy (ΔE^{QM}) of these perturbed structures was computed and then used in Equation 2, in which all the parameters are changed until the difference between force-field (ΔE^{FF}) and quantum mechanical energy is minimal.

$$(\Delta E^{QM} - \Delta E^{FF})^2 = \text{minimum} \qquad (2)$$

We have also investigated the dependence of the stretching and bending force constants on the stereochemistry of the compound by computing some parameters for the four *p*-menthan-3,9-diols under study (data not shown). The results indicated that the dependence of such parameters on the configuration of the chirotopic carbon atoms is negligible allowing to define a unique set of parameters (Table 1).

Results displayed in Table 1 show some relevant features. Thus, the force constants of the CA-CB and CC-CC bonds are 62 and 78 kcal/mol Å^2, respectively, lower than that of the CA-CA one, even although standard force-fields usually assign only one atom type to describe CA, CB and CC (Figure 1). On the other hand, the force constants of the CA-CB-H and CA-CC-H angles differ by 20 kcal/mol rad^2. These results indicate that the chemical environment plays a crucial role in the parametrization of stretchings and bendings. The importance of these terms in force-field simulations was recently emphasized by Boresch and Karplus [20].

The torsional term has been parametrized using an approach in which only the nature of the two central atoms is considered. Accordingly, all the torsions $\{A_i\}$-B-C-$\{D_i\}$ associated with the central bond B-C have the same parameters. Energy profiles were

Table 2. Torsional parameters (V_n, in kcal/mol) for *p*-menthan-3,9-diols (atom types are indicated in Figure 1). The model molecules used in the parametrization are also indicated.

Dihedral	V_n	γ	n	Model molecule
-CA-CA-	0.9	0	1	Butane
	1.7	0	3	
-CA-CB-	0.3	0	1	Propanol
	1.7	0	3	
-CA-CC-	2.0	0	1	2-Methylbutane
	0.6	0	2	
	1.2	180	3	
-CB-OH-	0.8	0	1	Ethanol
	1.4	0	2	
	0.5	180	3	
-CC-CC-	0.6	0	1	2,3-Dimethylbutane
	0.3	0	2	
	1.9	0	3	
-CC-OH-	0.8	0	1	Ethanol
	1.4	0	2	
	0.5	180	3	

Table 3. Partial charges (in electron units) for the four *p*-menthan-3,9-diols investigated (atom numbers indicated in Scheme 2)

ATOM	1	2	3	4
C1	0.3142	0.3154	0.4483	0.5230
C2	−0.2782	−0.3168	−0.3061	−0.4657
C3	0.4080	0.3384	0.4273	0.5889
C4	0.0443	−0.0126	−0.3295	−0.2700
C5	−0.2337	0.0335	−0.0606	0.0812
C6	−0.1767	−0.2551	−0.1818	−0.2722
C7	−0.4971	−0.4676	−0.5720	−0.5143
H(-C7)	0.1140	0.1080	0.1260	0.1099
H(-C1)	−0.0170	−0.0189	−0.0075	−0.0506
H(-C2)	0.0872	0.1069	0.0693	0.0928
O(-C3)	−0.7355	−0.7420	−0.7229	−0.7819
H(-O-C3)	0.4212	0.4470	0.4343	0.4651
H(-C3)	−0.0455	−0.0095	−0.0130	−0.0426
C8	0.2320	0.2033	0.2704	0.2881
C9	0.2151	0.1221	0.1643	0.1035
H(-C9)	−0.0050	0.0161	0.0117	0.0320
O(-C9)	−0.7487	−0.6863	−0.7155	−0.7305
H(-O-C9)	0.4704	0.4459	0.4480	0.4647
C10	−0.5336	−0.3325	−0.3640	−0.5449
H(-C10)	0.1210	0.0797	0.0879	0.1267
H(-C8)	0.0039	−0.0510	0.0202	0.0182
H(-C4)	0.0209	0.0294	0.0848	0.0674
H(-C5)	0.0824	0.0146	0.0427	0.0061
H(-C6)	0.0509	0.0595	0.0431	0.0505

computed at the HF/6-31G(d) level considering small model molecules for the different rotations involved in *p*-menthan-3,9-diols. The torsional parameters were then computed using the PAPQMD strategy as was described in the previous works [18, 19]. The torsional energy parameters (V_n), the values of the phase angle (γ), the periodicity (n) and the model molecules used in the parametrization procedure are listed in Table 2.

Electrostatic and van der Waals terms

The electrostatic term is usually the most important term in a force-field, and consequently requires an accurate parametrization [21]. In this work we have used the strategy developed by Momany [22] according to which the electrostatic charges are derived by fitting the rigorously defined quantum mechanical Molecular Electrostatic Potential (MEP) to the coulombic monopole-monopole electrostatic potential. Table 3 lists the atomic charges obtained at the HF/6-31G(d) level for the four stereoisomers under study.

It is worth noting that there are some differences in the atomic charges of the four compounds investigated due to the chirotopic carbon atoms. For instance, the configuration of C3 introduces a drastic change in the atomic charge of the neighbour atom C4. Thus, the charge of C4 in **1** and **2** (with configuration 3*R*) differs by about 0.25–0.27 electron units (e.u.) with respect to the charge in **3** and **4** (with configuration 3*S*). On the other hand, the C3 and C10 atoms also present variations in the same range depending on the configurations of C3 and C8. Thus, the charge on C3 clearly depends on the configuration of C8 whereas a more complex behaviour must be associated to the charge of C10, which seems to depend on the configuration of both C3 and C8. These results clearly illustrate that electrostatic parameters depend not only on the chemical constitution but also on the stereochemistry. It should be emphasized that this feature is not taken into account by a number of universal force-fields, which assign atomic charges considering only the chemical constitution.

Van der Waals atomic parameters are quite transferable [21, 23] and depend mainly on the atomic number and degree of hybridization. Accordingly, the parameters related to the atom types displayed in Figure 1 were initially obtained from the AMBER li-

Table 4. Van der Waals parameters (R in Å; ε in kcal/mol) for *p*-menthan-3,9-diols (atom types are indicated in Figure 1)

Atom type	R	ε
CA, CB, CC	1.91	0.110
H	1.54	0.010
OH	1.65	0.150
HO	1.00	0.020

braries [15, 24]. However, some of such parameters were adjusted in order to improve the comparison between MM and quantum mechanical results (see the next section). More specifically, the van der Waals parameters *R* and ε of the H atom type were gradually increased and decreased, respectively, until the best concordance between the properties (geometries, frequencies of vibration and thermodynamical parameters) predicted by quantum mechanical and MM methods was obtained. The resulting values were 0.05 Å (*R*) and 0.006 kcal/mol (ε) larger and smaller, respectively, than those reported in the AMBER forcefield [15]. The van der Waals for all the atom types described in Figure 1 are listed in Table 4.

Test cases

In order to validate the quality of the parameters listed in Tables 1-4, the optimized geometries, frequencies of vibration, heat capacities (constant volume) and molecular entropies computed from MM calculations were compared with those obtained from ab initio quantum mechanical calculations. For this purpose, the conformational preferences of **1**, **2**, **3** and **4** were investigated using both ab initio HF/6-31G(d) and MM methods. The conformational flexibility of these compounds arises from the possibility of ring inversion and rotation of the 1-methyl-2-hydroxyethyl and hydroxyl substituents. The possible staggered rotational isomers for these groups are 9 and 3, respectively, comprising a total of 54 rotamers if the two chair conformations are considered. Six of these rotamers, which were selected from pilot calculations at the semiempirical AM1 level [25], were used as starting geometries in HF/6-31G(d) and MM optimizations for each compound.

Table 5 compares the conformation of the lowest energy minimum predicted by MM and HF/6-31G(d) calculations for the four molecules under study. It is

Table 6. Maximum life-time of both intramolecular (τ_{intra} in ps) and intermolecular (τ_{inter} in ps) hydrogen bonds and the maximum time without forming hydrogen bonding interactions (τ_{free} in ps) for the two hydroxyl groups of the four *p*-menthan-3,9-diols.

Compound	Hydroxyl Group[a]	τ_{intra}	τ_{inter}	τ_{free}
1	C9-OH…O	2	31	4
	C9-O…HO	27	20	4
	C3-OH…O	27	34	3
	C3-O…HO	2	20	1
2	C9-OH…O	0	19	4
	C9-O…HO	1	16	5
	C3-OH…O	1	21	2
	C3-O…HO	0	23	1
3	C9-OH…O	0	31	6
	C9-O…HO	0	15	3
	C3-OH…O	0	27	4
	C3-O…HO	0	19	1
4	C9-OH…O	34	22	6
	C9-O…HO	50	18	1
	C3-OH…O	50	19	4
	C3-O…H O	34	20	3

[a] *n*-OH…O and C*n*-O…HO indicate that the hydroxyl group attached to the carbon atom *n* (see Scheme 2) acts as a donor and an acceptor, respectively.

worth noting that the two computational methods predict the same conformation in all the cases. Thus, the deviation between the HF/6-31G(d) and MM endocyclic dihedral angles is almost negligible. Moreover, the conformations predicted by MM for the exocyclic groups are similar to the ab initio ones, the average deviations for the dihedral angles C3-C4-C8-C10, C3-C4-C8-C9, C4-C8-C9-O, C8-C9-O-H and C2-C3-O-H being 19.1°, 12.2°, 8.3°, 91.8° and 12.3°, respectively. Thus, a very reasonable result is obtained for all the dihedral angles with exception of C8-C9-O-H. However, it is reasonable to assume that this will not give rise to errors in MD simulations since such torsion is expected to be quite flexible at room temperature. On the other hand, an intramolecular hydrogen bond between the two hydroxyl groups was found for the lowest energy minimum predicted at the HF/6-31G(d) level of both **1** and **4**. This interaction is also predicted by MM calculations, the geometrical parameters predicted at the two levels of theory being very similar.

Table 5 also compares the heat capacity and molecular entropy (T = 298 K) computed from MM with those obtained at the HF/6-31G(d) level. As it

Table 5. Lowest minimum energy conformation (dihedral angles in degrees) predicted for the four *p*-menthan-3,9-diols obtained from quantum mechanical calculations at the HF/6-31G(d) level and molecular mechanics calculations with the developed parameters. Heat capacities (in cal/mol) and entropies (in cal/mol K) at 25 Å are also indicated

Parameter	1		2		3		4	
	HF	MM	HF	MM	HF	MM	HF	MM
C1-C2-C3-C4	−56.6	−55.7	−56.2	−53.5	−57.5	−53.8	−55.9	−52.3
C2-C3-C4-C5	57.3	54.8	56.0	51.6	58.0	55.0	54.0	52.0
C3-C4-C5-C6	−57.9	−54.3	−56.7	−52.9	−56.9	−56.0	−54.5	−54.2
C4-C5-C6-C1	57.9	54.8	56.8	55.8	55.0	55.2	56.1	56.3
C5-C6-C1-C2	−53.7	−53.7	−53.8	−55.3	−53.1	−52.8	−54.2	−54.3
C6-C1-C2-C3	53.2	54.1	54.0	54.4	54.5	52.5	54.5	52.5
C3-C4-C8-C10	92.2	128.0	−73.6	−65.5	80.6	80.3	47.1	79.2
C3-C4-C8-C9	−114.4	−134.4	157.9	166.3	−43.9	−47.9	170.2	−153.9
C4-C8-C9-O	73.0	82.5	72.4	87.1	−54.6	−45.7	−174.0	−174.2
C8-C9-O-H	−177.7	127.9	177.6	74.9	−174.4	−74.7	−179.9	65.0
C2-C3-O-H	−160.6	−158.8	−156.9	−149.8	−129.6	−144.3	172.2	144.2
Cv	48.3	48.7	49.4	48.8	48.4	47.8	49.2	48.8
S	108.4	108.9	113.5	110.8	110.0	106.8	112.7	108.9

can be seen there is an excellent agreement between quantum mechanical and force-field thermodynamic parameters, the largest error being about 3%.

On the other hand, comparison of the local minima provided by both HF/6-31G(d) and MM indicates an excellent agreement between the two methods in both conformations and relative energies (data not shown). Regarding to bond lengths and angles, it is remarkable that the MM optimized ones deviate on average less than 0.03 Å and 3° from the quantum mechanical ones (data not shown). The frequencies of vibration of the investigated stereoisomers obtained from MM were compared with those from HF/6-31G(d). The correlation between MM and quantum mechanical frequencies was almost perfect ($r > 0.98$). Furthermore, the scaling coefficient arising from such correlation indicated that the MM frequencies are underestimated by about 6–12% with respect to the HF/6-31G(d) ones. This is a very reasonable result since it is well known that ab initio HF overestimates the rigidity of bonds and angles.

Molecular dynamics simulations

Computational procedure

Calculations were performed with the Amber 4.0 computer package [26]. We began the simulations using the lowest energy conformation found in the conformational search described in the previous section. Each compound was immersed into a box of water molecules having a density of 1 g ml, taken from a previous Monte Carlo equilibrium simulation. The water molecules that overlapped the *p*-menthan-3,9-diols were discarded. The resulting systems had dimensions of $17.17 \times 16.11 \times 15.24$ Å^3, and contained 121 water molecules. Periodic boundary conditions were applied, using the nearest image convention.

The force-field parameters used for the *p*-menthan-3,9-diols were those listed in Tables 1–4. The water molecules were described by the TIP3 model [27]. We imposed a 8 Å cutoff for nonbonded interactions, and updated the list of these interactions every 25 steps. The SHAKE algorithm [28] was used to constrain bond lengths of the solvent molecules to their equilibrium values.

The initial structure was subjected to 3000 steps of conjugate gradient energy minimization to relieve bad initial contacts. Molecular dynamics simulations were begun, starting with initial velocities set to zero. The systems were coupled to a thermal bath using the algorithm developed by Berendsen et al. [29] which applies a velocity scaling at each step, and heated the system to 300 K in 25 ps using a temperature coupling parameter of 0.2 ps in a constant volume simulation. A time step of 1 fs was used, and the coordinates were

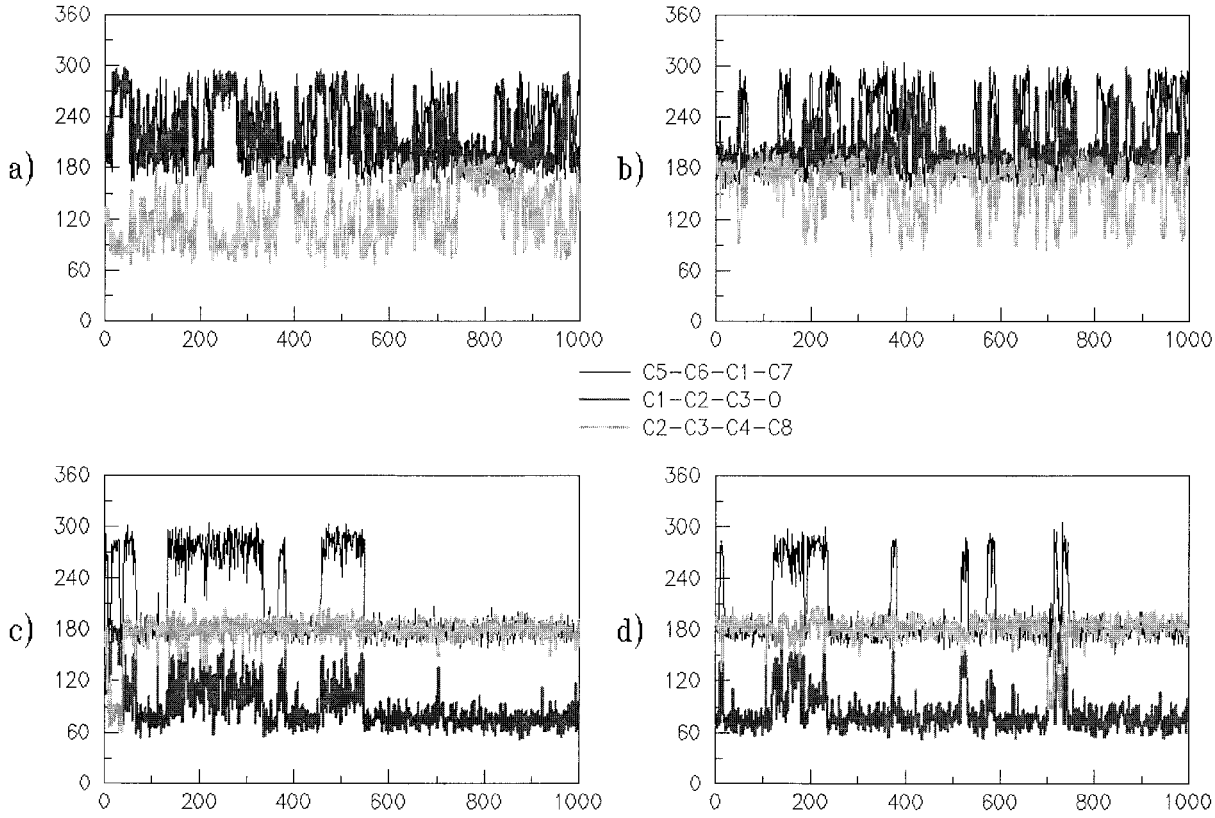

Figure 2. Evolution of the dihedral angles C5-C6-C1-C7, C1-C2-C3-O and C2-C3-C4-C8 along the simulation time for **1** (a), **2** (b), **3** (c) and **4** (d).

saved every 1 ps. Each simulation was run for a total of 1000 ps after 25 ps of equilibration.

Conformation of the cyclohexane ring

The MD simulations of the four *p*-menthan-3,9-diols investigated have been analyzed in order to ascertain their conformational preferences in aqueous solution. The three substituents of the cyclohexane ring in **1** and **2** are in *trans*, i.e. *all* three substituents occupy the same position which can be axial or equatorial depending on the conformation of the ring. The evolution of the C5-C6-C1-C7, C1-C2-C3-O and C2-C3-C4-C8 dihedral angles along the simulation time for these two compounds is displayed in Figure 2. Results clearly show that the three substituents alternatively visit both the axial and equatorial positions indicating that the simulations have efficiently explored the conformational space of these compounds.

As it can be seen in Figure 2a, for **1** the axial position is more populated than the equatorial one. Moreover, the three substituents present such axial arrangement at the same time indicating that the cyclohexane ring preferentially presents a chair conformation. This is a surprising results since a chair conformation with the three substituents in equatorial position was expected as the most stable. This anomalous conformational behavior has been also found in sterically crowded *all-trans*-alkylcyclohexanes [30, 31]. However, in **1** the stabilization of the axial position is related with the formation of an intramolecular hydrogen bond rather than with the size of the substituents. Thus, the hydroxyl groups easily form an hydrogen bond, which will be described below, when the substituents adopts an axial position. On the other hand, both the axial and equatorial positions present similar populations for **2**, the latter position being slightly favored. This trend points out the large flexibility of the *p*-menthan-3,9-diols and is consistent with the poor tendency displayed by **2** to form intramolecular hydrogen bonds (see below). Accordingly, the results obtained for **1** and **2** indicate that the formation of intramolecular hydrogen bonds between the two hydroxyl groups is controlled by the stereochem-

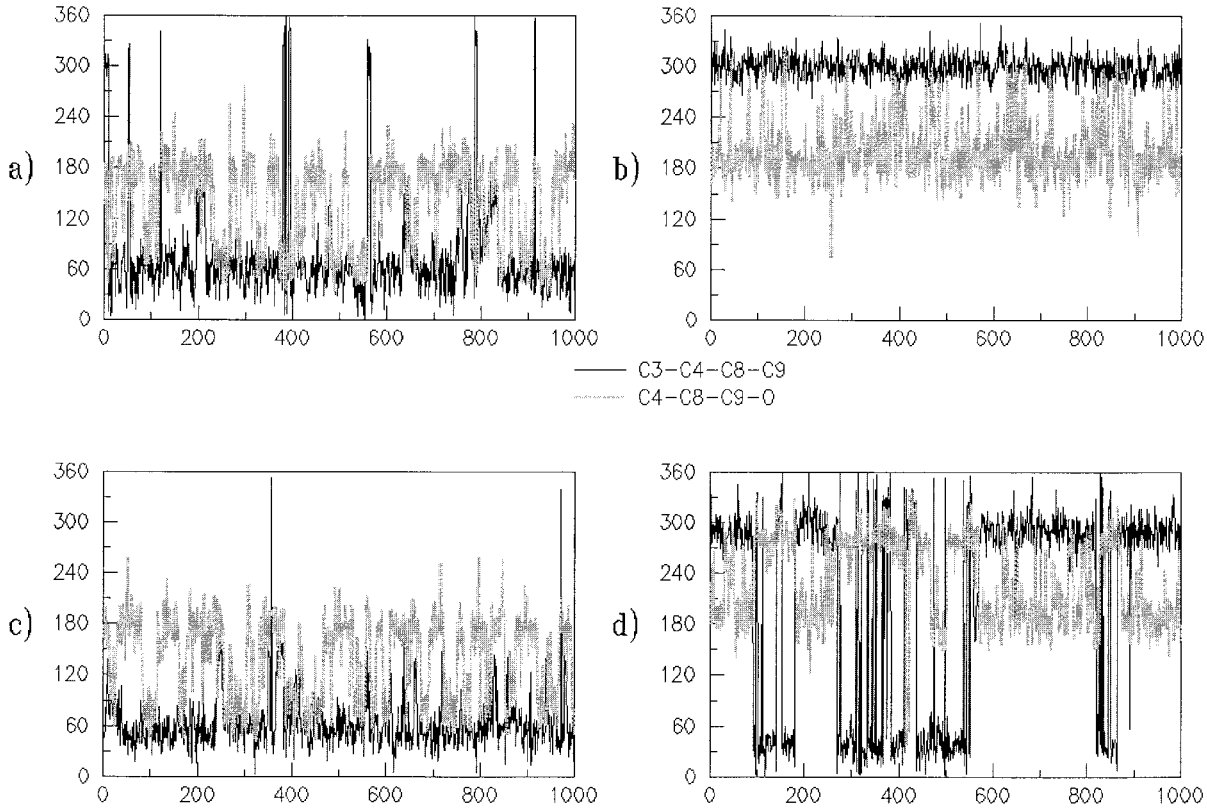

Figure 3. Evolution of the dihedral angles C3-C4-C8-C9 and C4-C8-C9-O along the simulation time for **1** (a), **2** (b), **3** (c) and **4** (d).

istry of C8 and such interactions drastically reduce the conformational flexibility of *p*-menthan-3,9-diols.

In **3** and **4** the substituents attached to C3 and C4 are in *cis*, both of them being in *trans* with respect to the methyl group attached to C1. Results displayed in Figures 2c and 2d reveal a very similar behavior for the two compounds, the equatorial position being clearly preferred for the bulky sustituent attached to C4. The hydroxyl group attached to C3 essentially remains in axial position indicating that the cyclohexane ring prefer a chair conformation. However, it should be noted that in some snapshots the ring deformed towards a twist conformation allowing an equatorial position to both the 1-methyl-2-hydroxyethyl and hydroxyl substituents. In this cases, the methyl group attached to C1 changes from an equatorial position to an axial one. By comparison with the stereochemistry of **1** and **2** it can be predicted that only **4** is able to form an intramolecular hydrogen bond between the hydroxyl groups. Inspection to the structures obtained from the trajectories of **3** and **4** allows to confirm such prediction (see below). Thus, the hydroxyl groups of **3** only interact with the solvent as was also found for **2**.

Conformation of the substituents

The conformational preferences of the 1-methyl-2-hydroxyethyl substituent were investigated by analyzing the evolution of the dihedral angles χ_1 (C3-C4-C8-C9) and χ_2 (C4-C8-C9-O) along the simulation time. Results for the four stereoisomers are displayed in Figure 3. As it can be seen, the conformational preferences of these angles are very similar for both **1** and **3**. Thus, χ_1 tends to adopt a *gauche*$^+$ conformation avoiding steric clashes between 1-methyl-2-hydroxyethyl substituent and the cyclohexane ring. The dihedral angle χ_2 can adopt both the *gauche*$^+$ and *trans* conformations, the former being compatible with the formation of the intramolecular hydrogen bond in **1**. On the other hand, the arrangement with χ_1 and χ_2 in *gauche*$^-$ and *trans*, respectively, is the dominant for **2**. Finally, **4** presents the largest flexibility in the 1-methyl-2-hydroxyethyl substituent. Thus, Figure 3d indicates that for χ_1 in addition to the predominant *gauche*$^-$ arrangement the *gauche*$^+$ one is also of certain relevance, whereas for χ_2 the conformation interchanges from *gauche*$^-$ to *trans*. It should

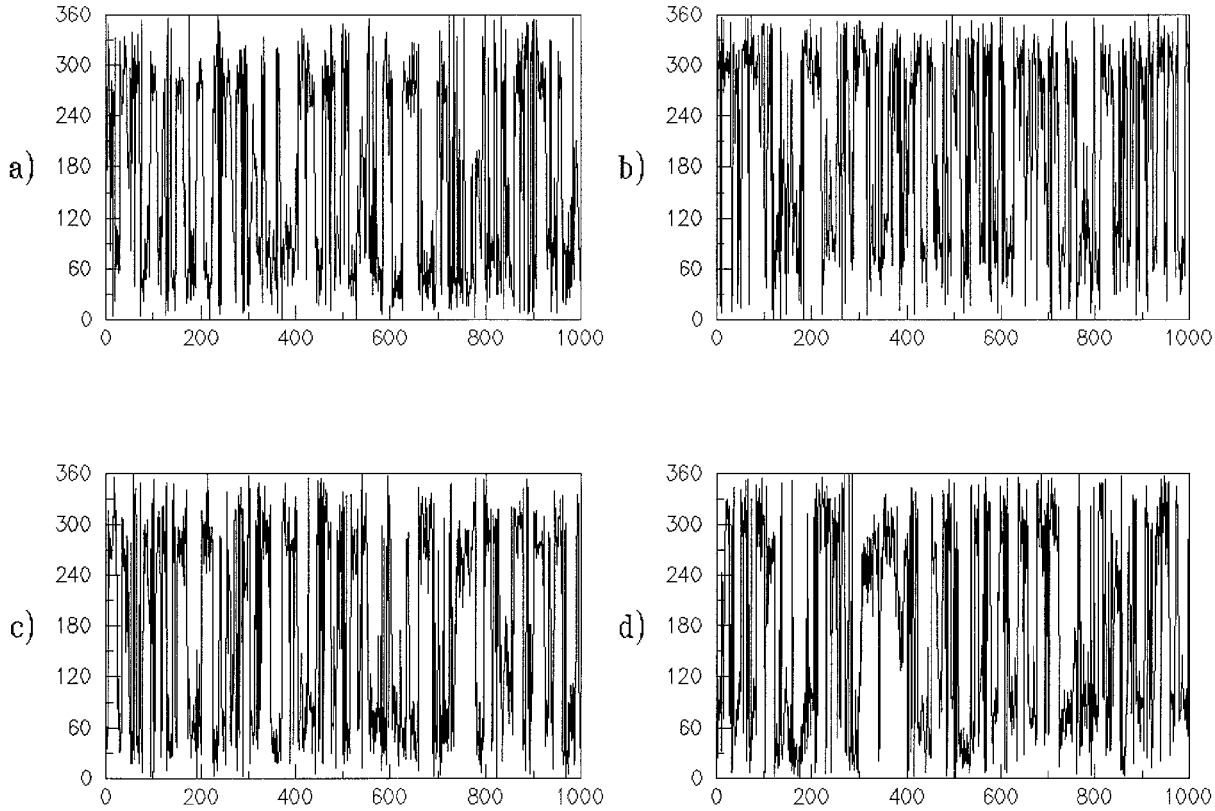

Figure 4. Evolution of the dihedral angle C8-C9-O-H along the simulation time for **1** (a), **2** (b), **3** (c) and **4** (d).

be noted that for this compounds the intramolecular hydrogen bond appears when both χ_1 and χ_2 are in *gauche*$^-$.

The analysis of the hydroxyl groups shows a very large conformational flexibility for the four compounds. This behaviour is illustrated in Figure 4, which displays the trajectory of the dihedral angle C8-C9-O-H. It should be emphasized that for **1** and **4** the hydroxyl groups remain around a certain arrangement during short periods of time, this feature being related with the formation of the intramolecular hydrogen bond.

Intramolecular and intermolecular hydrogen bonds

The analysis of the hydrogen bonds was performed considering both the two hydroxyl groups contained in the *p*-menthan-3,9-diols and the water molecules. A hydrogen bond was assumed if the OH...O distance is smaller than 2.5 Å. In Table 6 we list for the two hydroxyl groups of each compound the maximum life-time of both intramolecular (τ_{intra}) and intermolecular (τ_{inter}) hydrogen bonds and the maximum time without forming any hydrogen bonding interaction (τ_{free}). It should be mentioned that the average values for the H...O distance and the <O-H...O angle were 2.32 Å and 157° which point out the strength of the such interactions.

As it can be seen in Table 6, **2** and **3** show a common behavior. Thus, their hydroxyl groups only form hydrogen bonds with the solvent, being able to act as either donors or acceptors (Figure 5). The τ_{inter} ranges from 15 to 31 ps indicating that the residence time of the interacting molecules is very short. On the other hand, **1** and **4** are able to form both intra- and intermolecular hydrogen bonds (Figure 6). For **1** the values of τ_{intra} and τ_{inter} are quite similar and do not exceed a few tenth picoseconds. Instead, τ_{intra} is slightly larger than τ_{inter} for **4**, suggesting that for this compound forms the intramolecular interactions are stronger than the hydrogen bonds with the solvent molecules.

Results listed in Table 6 also show that there is no distinct variation of the maximum life-time for the interacting water with the configuration of the compound. Furthermore, we do not find a dependency of τ_{inter} on the chemical environment of the hydroxyl

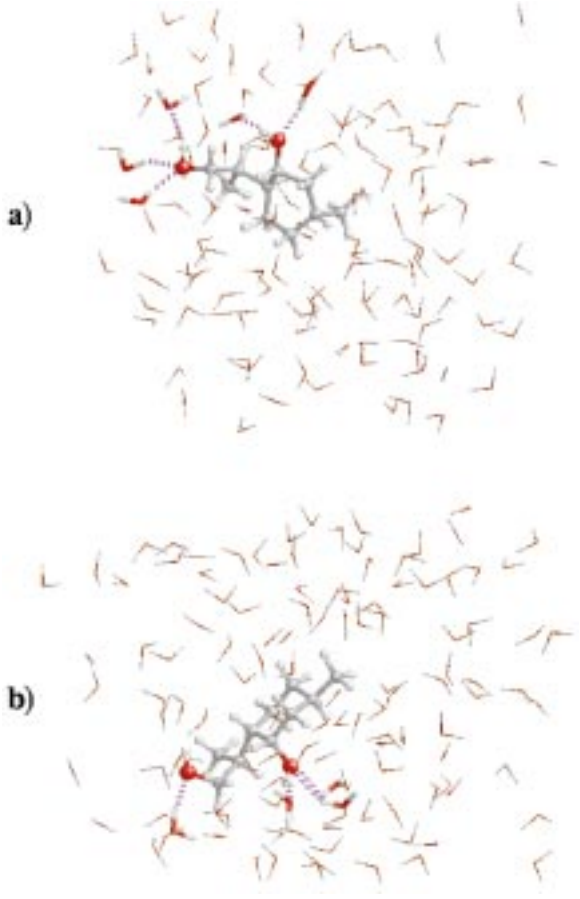

Figure 5. MD results for **2** (a) and **3** (b). Hydrogen bonds with the solvent are indicated.

group, i.e. the two hydroxyl groups present similar values. The small values of τ_{inter} are in opposition with the intuitive assumption that the hydrogen bonds between the solvent molecules and the polar groups, i.e. an energetically favorable interactions, should have very long life-times. Indeed, the very small values of τ_{inter} and τ_{free} indicate that the interacting water molecules have a large mobility and exchange very rapidly with the bulk water.

Conclusions

We have presented an explicit force-field parametrization for *p*-methan-3,9-diols. The new set of parameters were obtained from both semiempirical and ab initio quantum mechanical calculations. The reliability of these parameters have been tested by comparing the molecular geometries, frequencies of vibration, heat capacities and molecular entropies obtained from MM

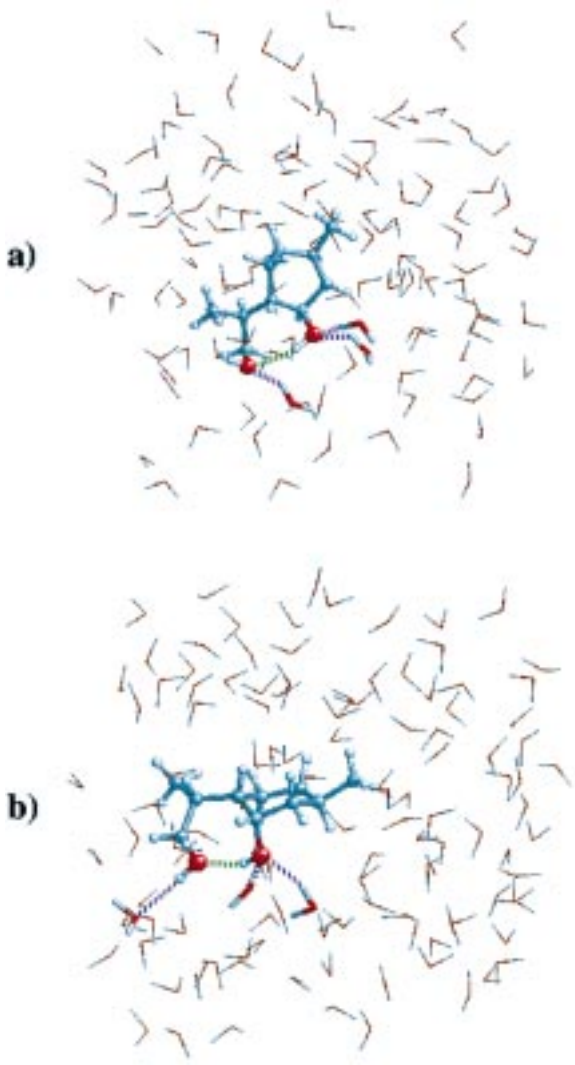

Figure 6. MD results for **1** (a) and **4** (b). Intra- and intermolecular hydrogen bonds are indicated.

with those computed at the HF/6-31G(d) level. MD simulations in aqueous solution have been performed for four different stereoisomers using the developed parameters. In all cases the cyclohexane ring tends to adopt a chair conformation, the axial or equatorial position of the substituents being defined in **1** and **4** by the formation of intramolecular hydrogen bonds. On the other hand, the life-times of both intra- and intermolecular hydrogen bonds are very short. This feature indicates that the hydroxyl groups present a large conformational flexibility.

Acknowledgements

The authors are indebted to the CESCA for computational facilities. The authors thank the Brazilian agencies FAPESP, CAPES and CNPq for financial support. A.M.N is grateful to FAPESP for a grant during her visit at the Universitat Politècnica de Catalunya.

References

1. Eliel, E.L., Allinger, N.L., Angyal, S.J. and Morrison, G.A., Conformational Analysis, Interscience, New York, 1965.
2. Loudon, G.M., Organic Chemistry, Cummings Publishing Company, Inc., 1988.
3. Perrin, C.L., Fabian, M.A. and Rivero, I.A., J. Am. Chem. Soc., 120 (1998) 1044.
4. Perrin, C.L., Fabian, M.A. and Armstrong, K.B., J. Org. Chem., 59 (1994) 5246.
5. León, S., Martínez de Ilarduya, A., Alemán, C., García-Alvarez, M. and Muñoz-Guerra, S., J. Phys. Chem., A101 (1997) 4208.
6. Brady, S., J. Am. Chem. Soc. 111 (1989) 5155.
7. Jansen, C.J., an Mey, D., Raabe, G. and Fleischhauer, J., J. Mol. Struct., 398 (1997) 395.
8. McCann, J.L., Rauk, A. and Wieser, H., Can J. Chem., 76 (1998) 274.
9. Foerster, G., Brezesinski, G., Neumann, S., Tschierske, C., Zaschke, H. and Kuschel, F., Mol. Cryst. Liq. Cryst., 193 (1990) 121.
10. Friedemann, R. and Naumann, S., J. Mol. Struct. (Theochem), 398 (1997) 405.
11. Dev, S., Terpenoids Handbook, CRC Press, Inc., Boca Raton: Florida, 1985.
12. Alemán, C. and Orozco, M., Biopolymers, 34 (1994) 941.
13. Alemán, C. and Muñoz-Guerra, J., Polym. Sci. Part B: Polym. Phys., 34 (1996) 963.
14. Alemán, C., Casanovas, J. and Galembeck, S.E., J. Comput. Aided Mol. Des., 12 (1998) 259.
15. Cornell, W.D., Cieplak, P., Bayli, C.L., Gould, I.R., Merz, A.R., Ferguson, D.M., Spellmeyer, D.C., Fox, T., Caldwell, J.W. and Kollman, P.A., J. Am. Chem. Soc., 117 (1995) 5179.
16. Hariharn, P.C. and Pople, J.A., Theor. Chim. Acta, 23 (1973) 213.
17. Dewar, M.J.S., Zoebisch, E.G., Healy, E.F. and Stewart, J.J.P., J. Am. Chem. Soc., 107 (1985) 3902.
18. Alemán, C., Canela, E.I., Franco, R. and Orozco, M., J. Comput. Chem., 12 (1991) 664.
19. Alemán, C. and Orozco, M., J. Comput. Aided Mol. Des., 6 (1992) 331.
20. Borech, S. and Karplus, M., J. Phys. Chem., A103 (1999) 103.
21. Orozco, M., Alemán, C. and Luque, F.J., Models Chem., 130 (1993) 695.
22. Momany, F.A., J. Phys. Chem., 82 (1978) 592.
23. O'Donnell, T.J., Rao, S.N., Koechler, K., Martin, Y.C. and Eccler, B.J., Comput. Chem., 12 (1991) 209.
24. Weiner, S., Kollman, P.A., Case, D.A., Singh, U.C., Ghio, C., Alagona, G., Profeta, S., Weiner, P., J. Am. Chem. Soc., 106 (1984) 765.
25. Dewar, M.J.S., Zoebisch, E.G., Healy, E.F. and Stewart, J.J.P., J. Am. Chem. Soc., 107 (1985) 107.
26. Pearlman, D.A., Case, D.A., Caldwell, J.W., Ross, W.S., Cheatham III, T.E., Ferguson, D.M., Seibel, G.L., Singh, U.C., Weiner, P.K. and Kollman, P.A., Amber 4.1, University of California, San Francisco, 1985.
27. Jorgensen, W.L., J. Chem. Phys., 77 (1977) 4156.
28. Ryckaert, J.-P., Ciccotti, G., Berendsen, H.J.C., J. Comput. Phys., 23 (1977) 327.
29. Berendsen, H.J.C., Postma, J.P.M., van Gunsteren, W.F., DiNola, A. and Haak, J.R., J. Chem. Phys., 81 (1984) 3684.
30. Goren, Z. and Biali, S.E., J. Am. Chem. Soc., 112 (1990) 893.
31. Golan, O., Goren, Z., Biali, S.E., J. Am. Chem. Soc., 112 (1990) 9300.